Available online at www.sciencedirect.com

SciVerse ScienceDirect

Journal of the European Ceramic Society 32 (2012) 511–516

www.elsevier.com/locate/jeurceramsoc

Original article

Effect of intergranular phase chemistry on the sliding-wear resistance of pressureless liquid-phase-sintered α-SiC

E. Ciudad, O. Borrero-López, F. Rodríguez-Rojas, A.L. Ortiz*, F. Guiberteau

Departamento de Ingeniería Mecánica, Energética y de los Materiales, Universidad de Extremadura, Badajoz, Spain

Received 16 March 2011; received in revised form 2 September 2011; accepted 12 September 2011
Available online 5 October 2011

Abstract

The effect was investigated of the intergranular phase chemistry on the sliding-wear resistance of pressureless liquid-phase-sintered (PLPS) α-SiC densified with 10 vol.% $5Al_2O_3 + 3RE_2O_3$ (RE = La, Nd, or Yb) additives. It was found that the sliding-wear behaviour of these ceramics is similar to what is observed in other polycrystalline ceramics: initial mild, plasticity-controlled wear followed by severe, fracture-controlled wear, with a well-defined wear transition. Most importantly, the sliding-wear resistance of PLPS SiC is found to increase with decreasing size of the RE^{3+} cation in the rare-earth oxide additive, with a lower susceptibility to mild and severe wear and a delayed transition to severe wear. Underlying this effect is likely the hardening of the intergranular phase resulting from the increase in the field strength of the RE^{3+}–O^{2-} bonds as the size of the RE^{3+} cation decreases. Tailoring the intergranular phase chemistry via the selection of RE_2O_3 sintering additives with cations as small as possible thus emerges as a potentially interesting approach to improving the sliding-wear resistance of PLPS SiC ceramics.

Keywords: SiC; Sintering; Wear resistance

1. Introduction

Silicon carbide (SiC) has inherent high strength, stiffness, hardness, and wear resistance. In addition, it is chemically stable, and possesses a high thermal conductivity and an elevated melting point.[1–5] This combination of physicochemical properties makes SiC-based materials attractive for use in contact-mechanical and tribological applications, such as bearings, wear-parts, valves, and seals.

Underlying the properties of SiC is the highly covalent nature of the Si–C bonds, which unfortunately also results in very low sinterability. Indeed, densification of SiC powders always requires the use of sintering additives. Depending on the nature of these additives, densification may take place by either a solid-state or a liquid-phase sintering mechanism. Traditionally, densification of SiC ceramics has been achieved via solid-state sintering by hot-pressing using small amounts of B and C as additives.[6] However, the elevated sintering temperatures and pressures required make this sintering route costly, and in addition it requires tedious and costly post-sintering machining processes to shape the final component. In liquid-phase sintering, however, the additives – generally combinations of aluminum oxide and rare-earth oxides[2,7–10] – melt during the heat treatment, thus enabling densification not only at lower temperatures, but also, and more importantly, under pressureless conditions. This allows low-cost SiC-based ceramics with near-net shape to be straightforwardly obtained.

The sliding-wear behaviour of SiC-based ceramics typically consists of initial mild, plasticity-controlled wear followed by severe, fracture-controlled wear, with a well-defined wear transition, as is commonly observed in other polycrystalline ceramics.[11–16] The wear resistance can be improved by optimizing the tribosystem (i.e., use of lubricants, etc.), and/or via microstructural design. Previous studies focused on the latter approach have suggested the following guidelines for the processing of highly wear-resistant pressureless liquid-phase-sientered (PLPS) SiC ceramics: (i) grain refinement;[17] (ii) grain elongation;[18,19] (iii) reduction of intergranular phase content;[17] and (iv) intergranular phase hardening by incorporation of nitrogen.[20] However, the chemical composition of the intergranular phase has attracted less

* Corresponding author. Tel.: +34 924289600x86726; fax: +34 924289601.
E-mail addresses: alortiz@materiales.unex.es, alortiz@unex.es (A.L. Ortiz).

0955-2219/$ – see front matter © 2011 Elsevier Ltd. All rights reserved.
doi:10.1016/j.jeurceramsoc.2011.09.011

attention, despite it is also being expected to influence the wear performance of PLPS SiC because the SiC grains are embedded in it. Indeed, Zhou et al.[10] have shown that the intergranular phase chemistry has a marked effect on other mechanical properties (elastic modulus, hardness, flexural strength, and toughness), some of which are very relevant for wear performance.

Based on the above, the present work was aimed at investigating the effect of the intergranular phase chemistry on the sliding-wear resistance of PLPS SiC. To that end, PLPS α-SiC ceramics were processed using three different additive systems consisting of 10 vol.% $5Al_2O_3 + 3RE_2O_3$ with wide ranging RE^{3+} cation size (RE = La, Nd, and Yb), and their sliding-wear behaviour was tested under the ball-on-three-disk configuration – which is ideal for the study of microstructural effects – and then discussed qualitatively using a semi-mechanistic model with a view to extracting additional guidelines for the microstructural design of low-cost, wear-resistant SiC-based ceramics for tribological applications.

2. Experimental procedure

2.1. Processing

Fully dense PLPS SiC ceramics were prepared from three powder batches, each containing α-SiC (UF-15, H.C. Starck, Goslar, Germany) plus Al_2O_3 (AKP-30, Sumitomo Chemical Company, NY) and RE_2O_3 (RE = La, Nd, or Yb; Strem Chemicals, France) in a 5:3 molar ratio as sintering additives. The choice of these three rare-earth oxides is because they have proved effective in densifying SiC,[10] while allowing one to investigate the fundamental question of the influence of intergranular phase chemistry on the sliding-wear resistance of PLPS SiC because they are formed by lanthanoids of very different cation radii (La^{3+} = 1.061 Å; Nd^{3+} = 0.995 Å; Yb^{3+} = 0.858 Å).[10] The relative amounts of SiC and $(5Al_2O_3 + 3RE_2O_3)$ in each of the powder batches were designed to yield in all cases PLPS SiC ceramics with 90 vol.% SiC and 10 vol.% $RE_3Al_5O_{12}$ after sintering (henceforth PLPS SiC–RE). The powder batches were prepared using routine methods applicable to PLPS SiC ceramics, i.e., by successive steps of powder wet mixing/homogenization in ethanol (liquid-to-powder weight ratio of 8) without dispersant, drying the slurries while stirring, and deagglomeration by crushing. Compacts were made by uniaxial pressing (C, Carver Inc., Wabash, IN, USA) at 50 MPa, followed by isostatic pressing (CP360, AIP, Columbus, OH, USA) at 350 MPa. Pressureless sintering was performed in a graphite furnace (1000-3560-FP20, Thermal Technology Inc., Santa Rosa, CA, USA) at 1950 °C for 1 h in a flowing Ar-gas atmosphere of 99.999% purity. The as-processed samples were characterized using a scanning electron microscope (SEM; S-3600N, Hitachi, Japan) operated at 15 kV with secondary electrons. The microstructures were revealed by plasma etching with CF_4 + 4% O_2 gas for 2 h, and the average size of the SiC grains (measured as the grain length) in these two-phase ceramics was quantified by image analysis (AnalySIS, Olympus Soft Imaging Solutions GmbH, Germany) as reported elsewhere[21] on at least 300 grains from various SEM micrographs taken randomly.

2.2. Mechanical properties

2.2.1. Vickers indentation

Cross-sections of the sintered materials were ground and polished to a 1-μm finish using routine ceramographic methods. Vickers-indentation tests were performed on the polished specimens to evaluate their hardness (H) and toughness (K_{IC}). All Vickers-indentation tests were performed under ambient conditions using a hardness tester (MV-1, Matsuzawa, Tokyo, Japan) equipped with a Vickers diamond pyramid, with maximum load of 98 N, indentation load rate of 40 $\mu m\, s^{-1}$, and dwell time of 20 s. Ten separate indentations were performed for each material. Subsequently, the tested surface was gold-coated for the measurement of the length of the diagonal of the residual impression and the total length of the surface trace of the radial cracks under optical microscopy (Epiphot 300, Nikon, Japan). The hardness and the toughness were determined using standard formulae.[22,23]

2.2.2. Hertz indentation

Polished cross-sections of each material were gold-coated and subjected to Hertzian indentation. The Hertzian indentation tests were made on those surfaces normally in a universal testing machine (5535, Instron, Canton, MA) at a constant cross-head speed of 0.05 mm min^{-1} over a load range of 15–1000 N, using WC spheres of radii 7.94 and 4.76 mm, under ambient conditions. The contact radius of each residual impression was then measured under the optical microscope, and used to construct the indentation stress–strain curves. E was determined from the linear stretch of the indentation stress–strain curve using a standard formula.[24,25]

2.2.3. Wear

Several polished disks (7 mm diameter, 2 mm thickness) were core-drilled from the sintered materials for wear testing. Wear testing was performed under ambient conditions in a Falex multi-specimen tribometer (Faville-Le Vally Corp., Sugar Grove, IL) configured in the ball-on-three-disks geometry. In this testing geometry, a commercial, bearing-grade Si_3N_4 ball (NBD 200, Cerbec, East Granby, CT) of radius 6.35 mm rotates in contact with three disk specimens aligned with their surface normals in tetrahedral coordination relative to the rotation axis.[12] Paraffin oil (Heavy Grade, Fisher Scientific, Fair Lawn, NJ) was used as lubricant (viscosity at 40 °C of $\sim 3.4 \times 10^{-5}\, m^2/s$ or 34 cst) to avoid any tribological effect such as friction-induced heating or triboreactions, and thus to study the intergranular phase chemistry effect only. The contact load on each disk was 80 N and the rotation speed was 100 rpm, corresponding to a sliding velocity of $\sim 0.04\, m\, s^{-1}$. The wear tests were interrupted at intervals, and the diameters of the circular wear scars (D) on each disk were measured under the optical microscope (two orthogonal measurements per disk, 3 disks per ceramic), and used as quantification of the extent of wear damage. Finally, the wear damage at the microstructural level was observed under SEM.

3. Results

Fig. 1 shows SEM images representative of the microstructures of the three PLPS SiC–RE ceramics. It can be observed that the microstructure is independent of the RE_2O_3 sintering additive used in combination with Al_2O_3, and consists in the three cases of equiaxed SiC grains (grain size L ∼0.8–1 μm) embedded in an intergranular phase that is crystalline and has the $RE_3Al_5O_{12}$ stoichiometry, as demonstrated in a previous study.[26] It can also be seen that the three PLPS SiC–RE ceramics are fully dense because there is no evidence of residual porosity in the SEM images.

Table 1 lists the E, H, and K_{IC} values of the three materials investigated. It can be observed that PLPS SiC–Yb has the highest E and H values (405 and 21.4 GPa, respectively), followed by PLPS SiC–Nd (377 and 18.7 GPa, respectively), and lastly by PLPS SiC–La (365 and 17.2 GPa, respectively). Thus, there is a clear correlation between H–E and the size of the RE^{3+} cation in the RE_2O_3, with a lower cation size (La^{3+} = 1.061 Å, Nd^{3+} = 0.995 Å, and Yb^{3+} = 0.858 Å) resulting in a harder and stiffer material. The fracture mode was observed to be the same in the three materials, namely intergranular fracture, although the K_{IC} values did vary with the RE_2O_3. Furthermore, K_{IC} exhibits a trend with the size of the RE^{3+} cation in the RE_2O_3 opposite to that of E and H, with PLPS SiC–La being the toughest material (4.4 MPa $m^{0.5}$), followed by PLPS SiC–Nd (4.2 MPa $m^{0.5}$), and lastly by PLPS SiC–Yb (4.0 MPa $m^{0.5}$). The magnitude of H, E, and K_{IC} as well as their correlations with the size of the RE^{3+} cation in the RE_2O_3 are entirely consistent with previous observations by Zhou et al.[10]

Fig. 2 shows the sliding-wear curves – evolution of the wear scar diameter (D) with the sliding-wear time on a semi-logarithmic scale (log t) – for the three PLPS SiC–RE ceramics. It can be observed that they exhibit the typical sliding-wear behaviour which is commonly observed in other polycrystalline ceramics, i.e., an initial section that corresponds to the mild wear regime, followed by an abrupt transition to a second section that corresponds to the severe wear regime. One can observe clearly in Fig. 2 that PLPS SiC–Yb has the greatest wear resistance in the mild regime, followed by PLPS SiC–Nd, and lastly by PLPS SiC–La. PLPS SiC–Yb has also the greatest transition time from mild to severe wear (40 min), followed again by PLPS SiC–Nd (15 min), and lastly by PLPS SiC–La (10 min). Moreover, the sequence of wear resistance in the severe regime is the same as in the mild regime because the three severe-wear stretches have apparently the same slope in Fig. 2 but are nonetheless shifted towards greater wear times in the logarithmic scale. Overall, one can therefore say correctly that PLPS SiC–Yb is the most wear-resistant of the three materials prepared in this study, and that PLPS SiC–La is the least. Since the Yb^{3+}, Nd^{3+}, and La^{3+} cation sizes are 0.858, 0.995, and 1.061 Å, respectively, it can thus be concluded that the resistance of PLPS SiC to sliding wear increases with decreasing size of the RE^{3+} cation in the RE_2O_3.

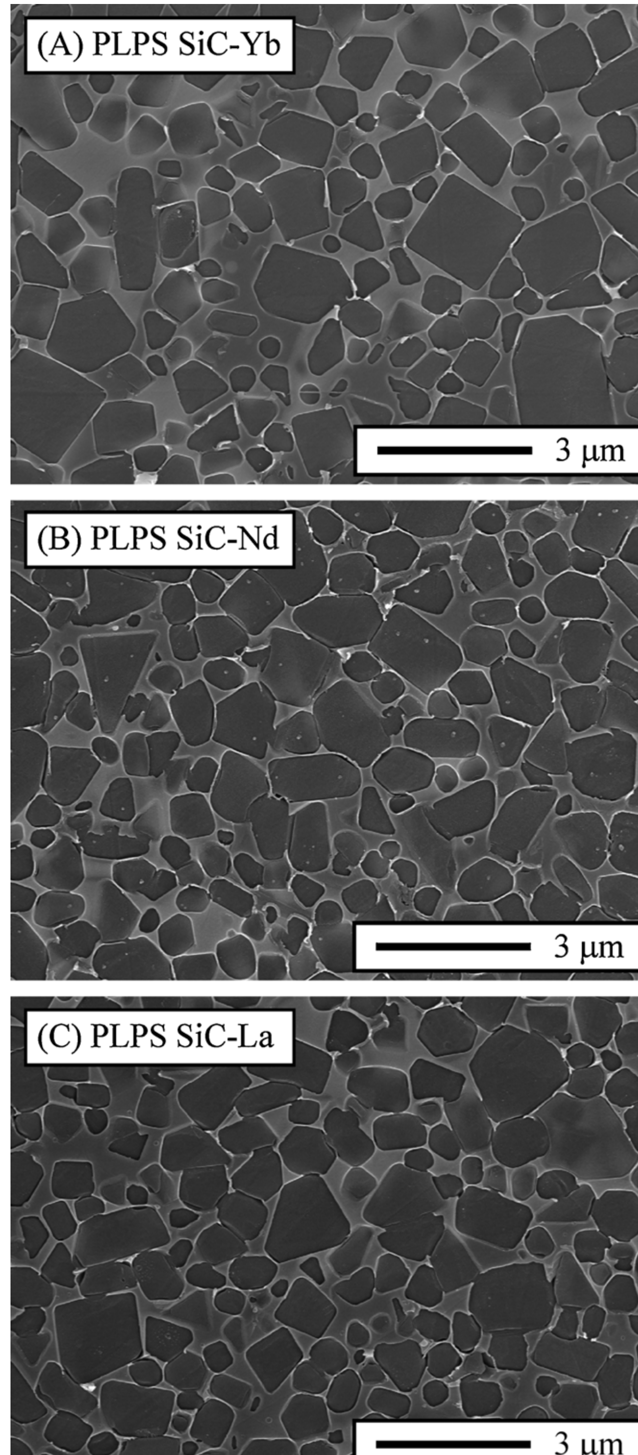

Fig. 1. SEM micrographs of the polished and plasma-etched cross-sections of the PLPS SiC ceramics fabricated with sintering aids (10 vol.%) of: (A) $5Al_2O_3$–$3Yb_2O_3$, (B) $5Al_2O_3$–$3Nd_2O_3$, and (C) $5Al_2O_3$–$3La_2O_3$.

Fig. 3 shows representative images of the damage at relevant scales at the end of the wear tests (1000 min of sliding time). Grooves and scratches caused by the asperities at the contact can be observed at the macroscopic level within the circular wear scar. Details observed under the SEM reveal severe damage at the microstructural level in the form of grain boundary fracture

Table 1
Mechanical properties of the three PLPS SiC–RE ceramics prepared in this study. The H and K_{IC} errors quoted are standard deviations; the E error is the standard error from the fit.

Sample; RE^{3+} cation size (Å)	Hardness, H (GPa; ±0.3)	Toughness, K_{IC} (MPa m$^{0.5}$; ±0.2)	Elastic modulus, E (GPa)
PLPS SiC–La; 1.061	17.2	4.4	365 ± 3
PLPS SiC–Nd; 0.995	18.7	4.2	377 ± 2
PLPS SiC–Yb; 0.858	21.4	4.0	405 ± 2

and grain pull-out within the grooves. This type of wear damage was common to the three PLPS SiC–RE ceramics, although it was most pronounced in PLPS SiC–La, then in PLPS SiC–Nd, and lastly in PLPS SiC–Yb.

4. Discussion

The results presented above reveal that the chemistry of the intergranular phase has a marked effect on the sliding-wear resistance of PLPS SiC ceramics processed with metal–oxide additives (i.e., $Al_2O_3 + RE_2O_3$). In particular, it was found that sliding-wear resistance increases – less susceptibility to mild and severe wear and a delayed transition from mild to severe wear – with decreasing size of the RE^{3+} cation in the RE_2O_3. The semi-mechanistic model proposed by Cho et al.,[12] which has been demonstrated to describe the sliding-wear behaviour of other polycrystalline ceramics including PLPS SiC,[11–20] can be used to justify qualitatively this effect. Briefly, during the mild-wear stage, tensile stresses (σ_D) accumulate as a function of sliding time at the SiC grains/intergranular phase interfaces as a consequence of dislocation plasticity in the SiC grains and especially in the softer intergranular phase, and add to the residual tensile stress induced during the processing itself (q). When at a certain critical sliding time (t_c) the stress intensity factor ($K(t)$) due to these accumulating stresses on pre-existing grain-boundary flaws exceeds the grain boundary toughness (K_{GB}), grain-boundary fracture and subsequent grain pull-out takes place, thereby leading to rapid material removal in the severe-wear stage. The time-dependent stress-intensity factor due to the pre-existing flaws can be written as:[12]

$$K(t) = \psi(\sigma_D(t) + q)\beta L^{0.5} \quad (1)$$

where L is the grain size, and the constants ψ and β are the crack geometry parameter and a scaling coefficient (≤1), and thus the condition for grain-boundary fracture is given by:

$$K_{GB} = K(t_c) = \psi(\sigma_D(t_c) + q)\beta L^{0.5} \quad (2)$$

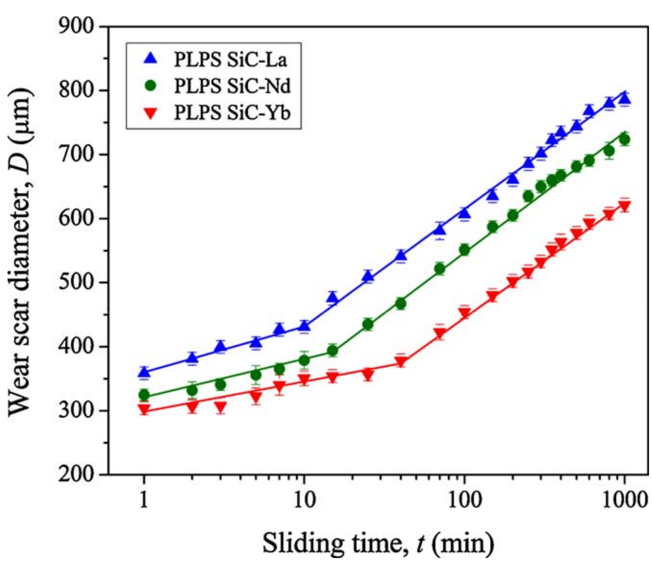

Fig. 2. Wear curves – wear scar diameter as a function of the sliding time – for the PLPS SiC–Yb, –Nd, and –La ceramics. Each datum point is the mean of three specimens tested; error bars represent data dispersion. The solid lines are to guide the eye, with the discontinuities in the lines indicating the mild to severe wear transition.

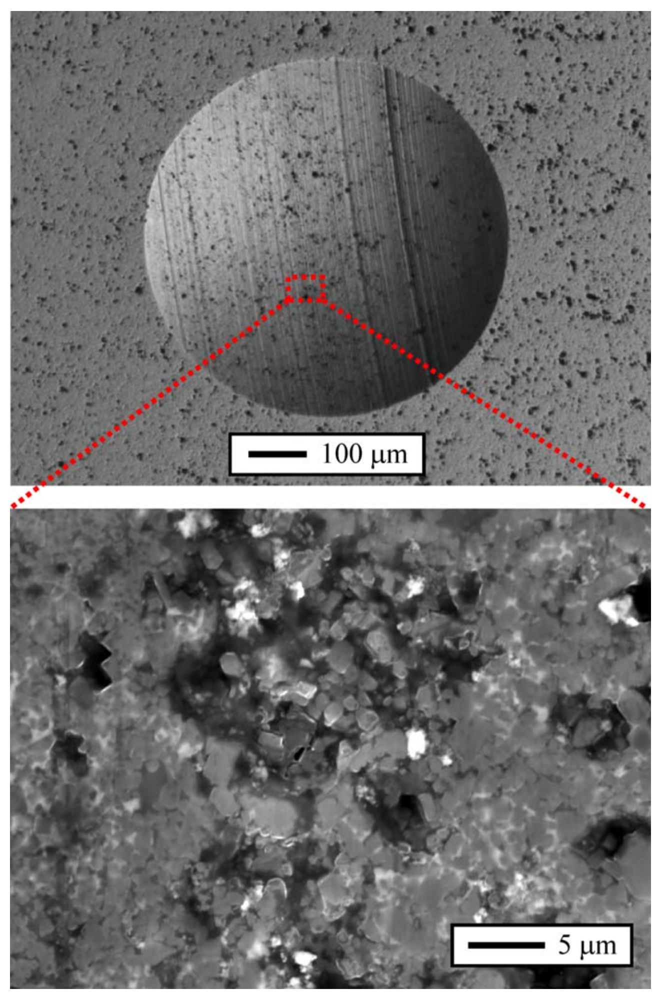

Fig. 3. Micrographs of the damage after 1000 min of sliding wear in PLPS SiC–Yb at the macroscopic and microstructural levels.

Within this framework, and given that the three PLPS SiC–RE ceramics fabricated in this study have the same grain size, the differences observed in the wear curves can only be attributed to the change in: (i) σ_D, which conditions the rate of mild wear and also affects the transition time from mild to severe wear; (ii) q; and/or (iii) K_{GB}, which affect the transition time only. In regards to the first point, the rate at which dislocation plasticity accumulates in a PLPS SiC ceramic depends on the hardness of the SiC grains and of the intergranular phase,[18,19] particularly this latter because it is the connected phase and is much softer than SiC.[27] The Vickers tests performed in the present study showed that the hardness of the PLPS SiC–RE ceramics increases with decreasing size of the RE^{3+} cation in the RE_2O_3. Since the SiC grains have the same size in the three PLPS SiC–RE ceramics and therefore the same hardness according to the Hall–Petch relationship, it can be concluded that the hardness of the $RE_3Al_5O_{12}$ intergranular phase increases with decreasing size of the RE^{3+} cation. This conclusion is entirely consistent with the consideration of the field strength of the Yb^{3+}–O^{2-}, Nd^{3+}–O^{2-}, and La^{3+}–O^{2-} bonds, as the three $RE_3Al_5O_{12}$ phases have the Al^{3+}–O^{2-} bonds in common. Note that, because the field strength of the RE^{3+}–O^{2-} bond is given by the expression $Z_aZ_ce^2/r^2$,[28] with Z_a and Z_c being the anion and cation charges, respectively, e the electron charge, and r the sum of the cation and anion radii, it increases as the size of the RE^{3+} cation decreases. A harder intergranular phase will reduce the rate at which plasticity-induced stress is accumulated during the wear of the PLPS SiC ceramics, thereby explaining the improved mild-wear resistance observed with decreasing size of the RE^{3+} cation in the RE_2O_3. A similar effect has been observed before in PLPS SiC ceramics with $Y_3Al_5O_{12}$ intergranular phase, in which the intergranular phase hardening achieved by the incorporation of nitrogen during sintering in a N_2-rich atmosphere resulted in improved wear resistance.[20]

The slower accumulation of plasticity-induced stress resulting from the increase in hardness with decreasing size of the RE^{3+} cation in the RE_2O_3 is in turn deemed principally responsible for the delayed transition from mild to severe wear because the simple appreciation of the magnitude of the K_{GB} and q effects suggests that these would be second-order corrections. Thus, the Hertzian curves of Fig. 4 do not reveal great differences in the contact pressure required to cause microcracking of the grain boundaries,[24,29] suggesting that K_{GB} increases little with decreasing cation radius. On the other hand, q not only is typically one order of magnitude smaller than $\sigma_D(t_c)$,[17] but also depends on the thermal expansion mismatch between the SiC grains and the oxide matrix,[30,31] and the thermal expansion coefficient of the rare-earth aluminum garnets (i.e., $RE_3Al_5O_{12}$) increases little with decreasing size of the RE^{3+} cation.[32] It is therefore reasonable to conclude that the increased hardness of the PLPS SiC ceramics with decreasing size of the RE^{3+} cation in the RE_2O_3 outweighs the effects of the small variations in K_{GB} and q, especially considering that the increase in K_{GB} would tend to delay the time for the transition from mild to severe wear whereas the increase in q would tend to shorten it. Finally, despite the fact that the wear mechanism in the severe-wear regime is far more complex, the improvement observed in this regime with decreasing size of the RE^{3+} cation in the RE_2O_3 is attributable essentially to the delayed transition to the severe-wear regime that reduces the severity of the abrasion by the wear debris trapped under the contact during sliding (i.e., lesser amount of abrasive and abrasive of larger size, as well as a shorter abrasion time for the same sliding time).

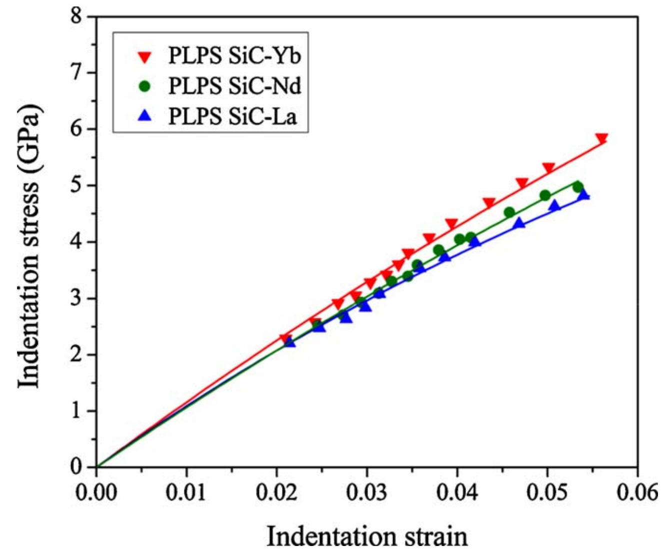

Fig. 4. Indentation stress–strain curves of the PLPS SiC–Yb, –Nd, and –La ceramics. Points are the experimental data, and solid curves are to guide the eye. The error bars are smaller than the dot size.

Based on the foregoing results and analyses, another processing guideline for improving the sliding-wear resistance of PLPS SiC ceramics would appear to consist of tailoring the intergranular phase chemistry through the selection of oxide additive systems with small metal cations so as to increase hardness. To create highly wear-resistant PLPS SiC ceramics for use in tribological applications, this novel processing guideline could be used in combination with the previously proposed guidelines of *in situ* nitride hardening[20] and reduction of intergranular phase content,[17] as well as with either that of grain refinement[17] or that of grain elongation[18,19] because these two guidelines are mutually exclusive. However, the processing of PLPS SiC ceramics that embodies all the above features remains a challenge for future work.

5. Conclusions

We have studied the effect of the intergranular phase chemistry on the sliding-wear resistance of PLPS α-SiC densified with 10 vol.% $5Al_2O_3 + 3RE_2O_3$ (RE = La, Nd, or Yb) additives. It was found that the sliding-wear resistance increases with decreasing size of the RE^{3+} cation in the RE_2O_3, with a lesser susceptibility to mild and severe wear and a delayed wear transition from mild to severe wear. This improvement in the wear resistance is likely to be caused by the increased hardness of the intergranular phase resulting from the decrease in the cation size in the RE_2O_3. Tailoring the intergranular phase chemistry via the selection of rare-earth oxides with small cation sizes thus emerges as another approach to improving the sliding-wear resistance in PLPS SiC ceramics. This new processing guideline can be used in combination with others formulated previously for a better microstructural design of low-cost, wear-resistant, SiC-based ceramics for tribological applications.

Acknowledgement

This work was supported by the Ministerio de Ciencia y Tecnología (Government of Spain) under Grant No. MAT 2010-16848.

References

1. Meetham GW, Van de Voorde MH. *Materials for high temperature engineering applications*. New York: Springer; 2000.
2. Padture NP. *In situ*-toughened silicon carbide. *J Am Ceram Soc* 1994;**77**(2):519–23.
3. Gahr K-HZ, Blattner R, Hwang D-H, Pöhlmann K. Micro- and macro-tribological properties of SiC ceramics in sliding contact. *Wear* 2001;**250**(1–12):299–310.
4. Sigl LS. Thermal conductivity of liquid phase sintered silicon carbide. *J Eur Ceram Soc* 2003;**23**(7):1115–22.
5. Schlesinger ME. Melting points, crystallographic transformation and thermodynamic values. In: Schneider Jr SJ, editor. *Engineered materials handbook*, vol. 4. ASM International; 1991. p. 883–91.
6. Prochazka S, Scanlan RM. Effect of boron and carbon on sintering of SiC. *J Am Ceram Soc* 1975;**58**(1–2):72.
7. Cordrey L, Niesz DE, Shanefield DJ. Sintering of silicon carbide with rare-earth oxide additives. In: Handwerker CA, Blendell JE, Kaysser WA, editors. *Ceramic transactions*. *Sintering of advanced ceramics*, vol. 7. Westerville, OH: American Ceramic Society; 1990. p. 618–36.
8. Pujar VV, Jensen RP, Padture NP. Densification of liquid-phase-sintered silicon carbide. *J Mater Sci Lett* 2000;**19**(11):1011–4.
9. Sigl LS, Kleebe H-J. Core/rim structure of liquid-phase-sintered silicon carbide. *J Am Ceram Soc* 1993;**76**(3):773–6.
10. Zhou Y, Hirao K, Toriyama M, Yamauchi Y, Kanzaki S. Effect of intergranular phase chemistry on the microstructure and mechanical properties of silicon carbide ceramics densified with rare-earth oxide and alumina additives. *J Am Ceram Soc* 2001;**84**(7):1642–4.
11. Borrero-López O, Ortiz AL, Guiberteau F, Padture NP. Microstructural design of sliding-wear-resistant liquid-phase-sintered SiC: an overview. *J Eur Ceram Soc* 2007;**27**(11):3351–7.
12. Cho S-J, Hockey BJ, Lawn BR, Bennison SJ. Grain-size and *R*-curve effects in the abrasive wear of alumina. *J Am Ceram Soc* 1989;**72**(7):1249–52.
13. Cho S-J, Moon H, Hockey BJ, Hsu SM. The transition from mild to severe wear in alumina during sliding. *Acta Metall Mater* 1992;**40**(1):185–92.
14. Wang YS, Hsu SM. Wear and wear transition mechanisms of ceramics. *Wear* 1996;**195**(1–2):112–22.
15. Wang X, Padture NP, Tanaka H, Ortiz AL. Wear-resistant ultra-fine-grained ceramics. *Acta Mater* 2005;**53**(2):271–7.
16. Thompson SC, Pandit A, Padture NP, Suresh S. Stepwise-graded Si_3N_4–SiC ceramics with improved wear properties. *J Am Ceram Soc* 2002;**85**(8):2059–64.
17. Borrero-López O, Ortiz AL, Guiberteau F, Padture NP. Effect of microstructure on sliding-wear properties of liquid-phase-sintered α-SiC. *J Am Ceram Soc* 2005;**88**(8):2159–63.
18. Borrero-López O, Ortiz AL, Guiberteau F, Padture NP. Improved sliding-wear resistance in *in-situ* toughened silicon carbide. *J Am Ceram Soc* 2005;**88**(12):3531–4.
19. Borrero-López O, Ortiz AL, Guiberteau F, Padture NP. Sliding-wear-resistant liquid-phase sintered SiC processed using α-SiC starting powders. *J Am Ceram Soc* 2007;**90**(2):541–5.
20. Borrero-López O, Ortiz AL, Guiberteau F, Padture NP. Effect of the nature of the intergranular phase on sliding-wear resistance of liquid-phase-sintered α-SiC. *Scripta Mater* 2007;**57**(6):505–8.
21. Xu H, Bhatia T, Deshpande SA, Padture NP, Ortiz AL, Cumbrera FL. Microstructural evolution in liquid-phase-sintered SiC. Part I. Effect of starting powder. *J Am Ceram Soc* 2001;**84**(7):1578–84.
22. Green DJ. *An introduction to the mechanical properties of ceramics*. Cambridge, UK: Cambridge University Press; 1998.
23. Anstis GR, Chantikul P, Marshall DB, Lawn BR. A critical evaluation of indentation techniques for measuring fracture toughness. I. Direct crack measurements. *J Am Ceram Soc* 1981;**64**(9):533–8.
24. Lawn BR. Indentation of ceramics with spheres: a century after Hertz. *J Am Ceram Soc* 1998;**81**(8):1977–94.
25. Padture NP. Hertzian Contacts. In: Cahn RW, Buschow KHJ, Flemings MC, Ilschner B, Kramer E, Mahajan, editors. *Encyclopaedia of materials: science and technology*. New York, NY: Pergamon Press; 2001. p. 3750–2.
26. Rodríguez-Rojas F, Ortiz AL, Guiberteau F, Nygren M. Oxidation behaviour of pressureless liquid-phase-sintered α-SiC with additions of $5Al_2O_3 + 3RE_2O_3$ (RE = La, Nd, Y, Er, Tm, or Yb). *J Eur Ceram Soc* 2010;**30**(15):3209–17.
27. Borrero-Lopez O, Pajares A, Ortiz AL, Guiberteau F. Hardness degradation in liquid-phase-sintered SiC with prolonged sintering. *J Eur Ceram Soc* 2007;**27**(11):3359–64.
28. Dietzel A. The cation field strengths and their relation to devitrifying process to compound formation and to the melting points of silicates. *Z Elektrochem* 1942;**48**(1):9–23.
29. Lawn BR, Padture NP, Cai H, Guiberteau F. Making ceramics "ductile". *Science* 1994;**263**(5150):1114–6.
30. Lawn BR, Padture NP, Braun LM, Bennison SJ. Model for toughness curves in two-phase ceramics. I. Basic fracture mechanics. *J Am Ceram Soc* 1993;**76**(9):2235–40.
31. Padture NP, Runyan JL, Bennison SJ, Braun LM, Lawn BR. Model for toughness curves in two-phase ceramics. II. Microstructural variables. *J Am Ceram Soc* 1993;**76**(9):2241–7.
32. Zinov'ev SY, Krzhizhanovskaya VA, Glushkova VB. Thermal expansion of rare-earth aluminum garnets. *Inorg Mater* 1987;**23**(4):630–2.